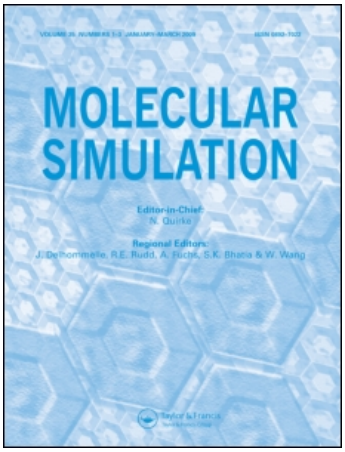

Molecular Simulation
Publication details, including instructions for authors and subscription information:
http://www.informaworld.com/smpp/title~content=t713644482

DNA Nano-Gears

Reza Mohammadzadegan[a]; Mohammad Hossein Sheikhi[a]
[a] Nanotechnology Research Institute, Shiraz University, Shiraz, Iran

To cite this Article Mohammadzadegan, Reza and Sheikhi, Mohammad Hossein(2007) 'DNA Nano-Gears', Molecular Simulation, 33: 13, 1071 — 1081
To link to this Article: DOI: 10.1080/08927020701541014
URL: http://dx.doi.org/10.1080/08927020701541014

Molecular Simulation, Vol. 33, No. 13, November 2007, 1071–1081

DNA Nano-Gears

REZA MOHAMMADZADEGAN* and MOHAMMAD HOSSEIN SHEIKHI†

Nanotechnology Research Institute, Shiraz University, Shiraz, Iran

(Received April 2007; in final form June 2007)

DNA is a nanoscale material for programmable self-assembly, using the selective affinity of pairs of DNA strands to form DNA nanostructures. Self-assembly is the spontaneous self-ordering of substructures into superstructures which driven by the selective affinity of the substructures. DNA self-assembly is the most advanced and versatile system that has been experimentally demonstrated for programmable construction of patterned systems on the molecular scale. This programmability renders the scaffolding have the patterning required for fabricating complex devices made of these components. We present various strategies to assemble DNA based gears for application in nano-machines, nano-motors and nano-devices. In this paper, some fundamental parts of mechanical nano-machines with DNA blocks are designed. These kinds of nanostructures, nano-gears, are fundamental for the development of future useful molecular-level devices.

Keywords: DNA Nanostructure; Self-assembly; Nano-machine; Nano-device; Nano-gear

1. Introduction

Nanotechnology refers to all technologies aiming to build objects, make measurements, and carry out processes on the nanometer length scale. In particular molecular nanotechnology exemplifies the bottom up approach, which is briefly defined as the ability to build nanostructures with molecular precision, such as molecular machinery. Machines and devices operating at the nanometer scale have wide variety of exquisite applications ranging from medicine to space flight, while dramatically reducing the energy and material requirements.

It has been widely projected that within approximately 10–20 years, traditional top-down fabrication methods for manufacturing devices will reach their resolution limits. Anticipating this crisis, the researchers in the field of nanoscience have begun developing bottom-up techniques for molecular assembly of nano-devices. One potential approach is to use self-assembling DNA nanostructures as scaffolds for constructing and positioning molecular-scale machines and devices [1] which provides a programmable methodology for bottom-up nanoscale construction [2]. The programmability is due to the highly specific hybridization of complementary DNA strands used to specify interactions both within and between DNA tiles [3,4].

DNA is organized as two complementary strands, with the hydrogen bonds between them. Each strand of DNA is a chain of chemical "building blocks", called nucleotides, of which there are four types: adenine (A), cytosine (C), guanine (G) and thymine (T), where A and G are purine bases and T and C are pyrimidine bases. Between the two strands, each base can only "pair up" with one single predetermined base: A + T, T + A, C + G and G + C are the only possible combinations. Two nucleotides paired together are called a base pair [5].

Two approaches to DNA-directed nano-block construction are based on using either DNA hairpins or DNA templates. DNA hybridization, without formation of covalent bonds, has been exploited in several cases for the parallel assembly of multiple building blocks into supramolecular nanostructures [6–9]. The building blocks for such materials can be made of DNA alone. Seeman *et al.* have built elegant branched structures, such as, a DNA cube and even more complex geometric designs have been constructed [2,10–12]. Extension of this work applying DNA tiles was made by Seeman *et al.* and LaBean *et al.* [13–16]. DNA-organic hybrids consisting of a bent organic backbone attached to two complementary DNA sequences were assembled to form polydisperse cyclic structures [17]. Bunz *et al.* demonstrated the formation of linear assemblies of organometallic

*Corresponding author. Tel/Fax: + 98-711-628-6602. Email: admin@nanodetails.com
†Tel/Fax: +98-711-628-6602. Email: msheikhi@shirazu.ac.ir

Molecular Simulation
ISSN 0892-7022 print/ISSN 1029-0435 online © 2007 Taylor & Francis
http://www.tandf.co.uk/journals
DOI: 10.1080/08927020701541014

compounds attached to two different DNA sequences at the termini [18]. DNA also has been demonstrated to be a useful material for mechanical devices [19–24]. In our recent paper [3], we described the design of the 3 × 3 and 5 × 5 DNA tiles that form DNA lattices with hexagonal and octagonal pores.

This article deals with processes, which include both DNA-programmed assembly and formation of covalent bonds between multiple building blocks to generate macromolecular nano-gears. The contributions to this field from other groups were described, but the main emphasis will be on our modular approach to the challenge of self-assembly and the concepts behind our work.

2. Methods

2.1 Basis of DNA nanostructures

The basic laws of the DNA nanotechnology were considered to design the sequences. Briefly, DNA molecules consist of two complementary chains of nucleotides which are ssDNAs (single stranded DNAs). Nucleotides are composed of a sugar, phosphate groups and a base. The base may be adenine, cytosine, guanine or thymine. Hydrogen bonds between the base pairs (A + T and G + C) hold the chains together.

Additionally, the design of branched nucleic acid motifs is based on the notion of maximizing the base pairing. In the present work, our designs were based on using DNA single strands and their efficient capability to bind their complementary strands, and or with their own complementary sequences. Distinctively, special highly ordered gear structures were designed due to the first method and other gear and cross shape structures were designed on the basis of the second system, which is called DNA folding.

2.2 The theoretical basis of DNA folding

The ssDNAs fold into specific three-dimensional conformations, which are determined by the sequence of nucleotides. The thermodynamic model for DNA structure formation posits that, out of the exponentially many possibilities, a DNA molecule folds into that structure with the minimum free energy (mfe) [25,26]. Free energy models typically assume that the total free energy of a given secondary structure for a molecule is the sum of independent contributions of adjacent, or stacked, base pairs in stems (which tend to stabilize the structure) and of loops (which tend to destabilize the structure). The change of free energy is $\Delta G = \Delta G^{o\prime} + RT\ln([B]/[A])$, whereas $\Delta G^{o\prime}$ is the standard free energy. A reaction can occur spontaneously only if ΔG is negative, and the more negative ΔG the more stability of the structure. A folded molecule is largely held together by the resulting set of bonds [27]. The ssDNAs also join each other into specific three-dimensional conformations, which are determined by the sequence of nucleotides. Again, the thermodynamic model for DNA structure formation posits that, out of the exponentially many possibilities, a DNA molecule folds into that structure with the minimum free energy (mfe) [25].

The melting temperature (T_m) of a double stranded DNA (dsDNA) is calculated as [28]

$$T_m = 69^\circ + 0.41(\%G + C) \quad (1)$$

In an assumed two-state model, in which denaturing has no intermediate, the steep part of the melting curve reflects the dsDNA to single strand equilibriums

$$\text{ssDNA} + \text{ssDNA} \leftrightarrow \text{dsDNA} \quad (2)$$

The association constant at the midpoint (when half of the DNA is single stranded and the other half is helical) is $k_{50} = 4/[\text{C}]$, where [C] is the sum of the concentrations of the two single strands which are non-self-complementary. Since, for any process at equilibrium, $\Delta G^\circ = -RT\ln K$ and $\Delta G^\circ = \Delta H^\circ - T\Delta S^\circ$ [29], we have

$$\Delta H^\circ - T\Delta S^\circ = -RT\ln K \quad (3)$$

where $R = 1.987$ cal. $\text{K}^{-1}\,\text{mol}^{-1}$. At the midpoint, $T = T_m$ and $K = K_{50}$. Therefore, for non-self-complementary strands,

$$\Delta H^\circ - T_m\Delta S^\circ = -RT_m\ln(4/[\text{C}]) \quad (4)$$

After rearranging terms, we get

$$1/T_m = R\ln[\text{C}]/\Delta H^\circ + (\Delta S^\circ - R\ln 4)/\Delta H^\circ \quad (5)$$

From the concentration dependence of the melting temperature, the standard enthalpy and entropy can be determined using so-called van't Hoff plot of $1/T_m$ versus ln [C] [30]. The standard free energy of duplex formation, ΔG°, at any temperature can then be determined. The total free energy change of a DNA helix from its individual strands is given by:

$$\Delta G^\circ(\text{total}) = \sum_i n_i\Delta G^\circ(i) + \Delta G^\circ(\text{init}\,w/\text{term GC}) + \Delta G^\circ(\text{init}\,w/\text{term AT}) + \Delta G^\circ(\text{sym}) \quad (6)$$

where $\Delta G^\circ(i) = \Delta H^\circ(i) - T\Delta S^\circ(i)$ are the standard free energy changes for the ten possible Watson–Crick base pairs, n_i is the number of occurrences of each type of base pairs, i, and $\Delta G^\circ(\text{sym})$ equals $+0.43\,\text{kcal}\,\text{mol}^{-1}$ if the duplex is self-complementary and zero if it is not self-complementary. To account for differences between duplexes with terminal AT versus terminal GC pairs, two initiation parameters are introduced. The calculations in this paper are based on the data in table 1 [25].

2.3 Molecular modeling

Modeling simulations were performed in vacuo to examine the puckering profiles of the nucleic acids (AMBER 99). This was done using the conformational search module in HyperChem with a conjugate gradient

Table 1. ΔH° (kcal/mol) and ΔS° (cal/K·mol) for nearest neighbor calculation. All values refer to forming duplex at 1M NaCl, 25°C, and pH = 7.0 [24].

Sequence	*ΔH°*	*ΔS°*
AA/TT	−8.4	−23.6
AG/CT	−6.1	−16.1
AT/AT	−6.5	−18.8
AC/GT	−8.6	−23.0
GA/TC	−7.7	−20.3
GG/CC	−6.7	−15.6
GC/GC	−11.1	−28.4
TA/TA	−6.3	−18.5
TG/CA	−7.4	−19.3
CG/CG	−10.1	−25.5
Initiation with one or two GC	0.0	−5.9
Initiation with AT only	0.0	−9.0
Symmetry correction	0.0	−1.4
5′ TA correction	0.4	0.0

limit of 0.01 kcal/A° mol. Endocyclic torsional variations were first treated systematically then simultaneously by applying the usage directed scheme with restricted ranges for ring torsion flexing in conjunction with a non-Metropolis criterion as described by Kollosvary and Guida [31]. High energy structures as well as those with relative energy differences within 0.05 kcal mol^{-1} were discarded in the post-optimization runs. All low energy conformers that fell within the specified acceptance criteria were further refined by a second series of optimizations in which only acyclic torsional parameters were varied and a lower gradient limit applied (0.0001 kcal/A° mol). The hardware we have used was dabble core Intel Pentium IV 3.00 GHz, with 1.5 Gb of Ram. Each modeling process has taken about 1000–2000 hours depending on the molecule sizes. The final modeled structures were studied and the figures were rendered with VMD 1.8.5 [32].

3. Results

3.1 Designing the sequences

General. Seven different structures were designed. Three of them were designed based on the first method, DNA templates, while the others were based on the second method, DNA hairpins. In all cases, present sticky ends were typically five bases long, and cohere with good fidelity.

3.1.1 The first method. *General*. In this method, as we previously discussed, the design of branched nucleic acid motifs was based on the notion of maximizing the base pairing. This method is assumed as DNA templated nanostructure engineering, where complementary ssDNAs join together to form the final structure, but without any hairpin formation. The sequences were complementary and would cohere with good fidelity. In the following sessions the formation of the appropriate structures were based on this method.

First structure. In the first structure, the sequences were consisted of mixed combinations of complementarity. The designed sequences were;

A; 5′-ATCGGGTAGGTCAGCATAACATGCGGGGG-TTTTCCAAATTCCATCTTGAATGCGCATTACAGGA-GGCGCATGGACACCGCACCAGAGGTAGCTACGA-CGATTTTGGGGCAT TAAAAAGCCTGCAAAAAGCC CGTATGGACCATCAACACGCGTAGTAATGGCCAA-TAAGGAGGACATTAG-3′

B; 5′-CATTTTTTACCTCTGGTGCGGTGTCCATGC-GCCTCCTGTAATGCGCATTCAAGGGGGCTAATGT-CCTCCTTATTGGCCATTACTACGCGTGTTGATGG-TC-3′

C; 5′-GCTTTTTGATGGAATTTGGAAAACCCCCG-CATGTTATGCTGACCTACCCGATGGGGGTACGGG-CTTTTTGCAGGCTTTTTAATGCCCCAAAATCGTC-GTA-3′

The first sequence (A) was main sequence and it was longer than the others. There was no internal complementarity in that sequence, but each domain of the sequence was complementary with the domains of the other sequences. There was also no complementarity within and between the other sequences. The result was formation of a 4-point star shape structure with four arms. As it is shown in figure 1, there were also four linker domains at the center of the structure. Those domains were designed to be used as linkers to join other structures; it would occur using their complementary sequences. Thus the whole structure would join other structures in nanoscale devices and machines.

Second structure. In the second structure, the sequences were consisted of mixed combinations of complementarity. The designed sequences were;

A; 5′-ACATCCTTTACCTTCCACCACTATTAATAA-ATCTGTCCATGATGAAGCCAACGTTAGGCACCCA-ATCTCCTCAATTAAGAGTCCCCGGTAGCAGTGGTA TGGACTTGTGTCTCAGCCGCCCAGATATTAGCA-CACGGTGCGGCGCAGTGTT-GACGGGGTCCGCCTGCCGGCGAGGGGGAGGT-TACTCGTGTGTCGTGAGAACGGTGCCTTGTTGT-TAGTAGCCCCCCGCAGTGGGGTTGCTGGTGTT-CAG-3′

B; 5′-GGCGGACCCCGTCACTCACCACTGTAGAG-AATTTTACCACTGCTACCGGGGAGTCTCTTTTGA-GGAGA-3′

C; 5′-GAGACACAAGTCCACAGACGCCACCACA-CGGACGTTGGCTTCATCATGGACAGATTTAAAAG-TGGTGG-3′

D; 5′-AAGGTAAAGGATGTGCAGCCAACCCATGT-CATTGATCTCACGACACACGAGTAACCTCCCCGC-CGGCA-3′

E; 5′-CAACAAGGCACCGTTCGAGACTTGCTCTC-CCCTACACTGCGCCGCACCGTGTGCTAATCGGGC-GGCTT-3′

F; 5′-TTGGGTGCCTAACGGGCTCCTGAATCGGC-CCCTGAACACCAGCAACCCCACTGCGGGGCTACT-AATAA-3′

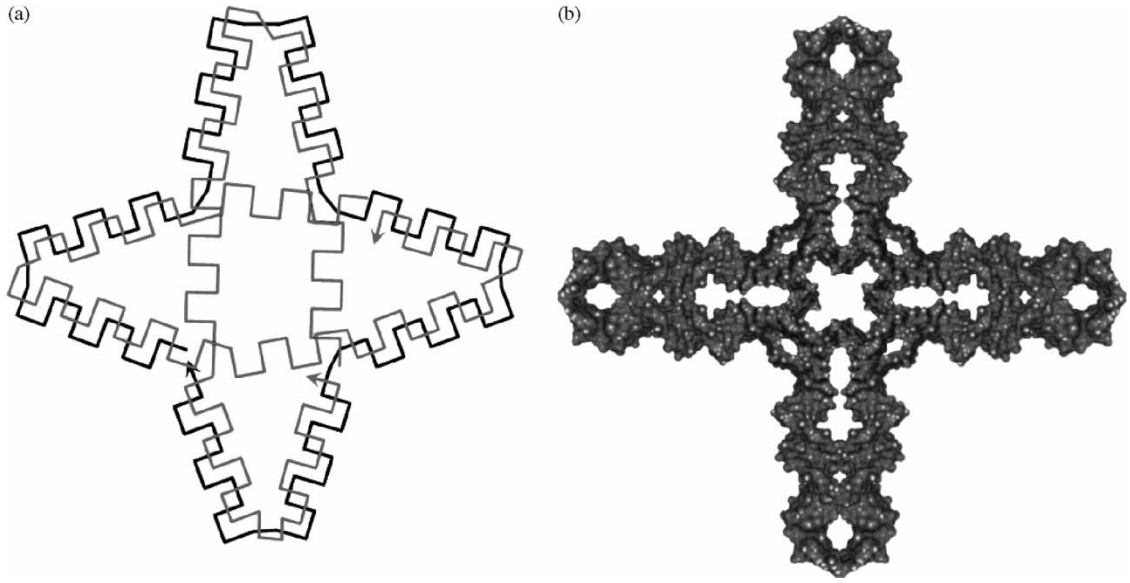

Figure 1. 4-Point star shape DNA nano gear. (a) The schematic view of three ssDNAs which bind with good fidelity and form a 4-point star shape structure. (b) The modeled structure which is consisted of those three ssDNAs. The 4-point star shape structure includes four arms and four linker domains at the center of the structure. The linker domains were designed to be used as linkers to join other structures; it would occur using their complementary sequences.

The first sequence (A) was main sequence and it was longer than the others. There was no internal complementarity in that sequence, but each domain of the sequence was complementary with the domains of the other sequences. There was also no complementarity within and between the other sequences. The result was formation of a 5-point star shape structure with five arms. As it is shown in figure 2, there were also five linker domains at the center of the structure. Those domains would also be used as linkers to join other structures.

Third structure. In the third structure, again the sequences were consisted of mixed combinations of complementarity. The designed sequences were;

A; 5′-ATCGCGTGCGACGCATGCAGTGCATGACG-AGGGCGCTTACCCCTCGCGACTGTACCAGGAAA-ATCCAGGAACCGACCCATTGTGTTTTACAAATCC-GCATGGTGCACCAGGGGCCCCCGCGCTGACCAT-TAAAATTCCGCGCTGCATGACTTTTGGGACC-3′

B; 5′-TTTTTTTTCTGCATGCGTCGCACGCGATGT-GTGTTGTTGCGAAGCGGAATTTTAATGGTCAGC GTAGGATGCCAGTGCATGCGGATTTGTAAAACA-CAGGGGGGGGGGGGGGGTCCTGGTACAGTCGC-GAGGGTTTTTTT-3′

C; 5′-TTTGGGAAGTAAGCGCCCTCGTCATGCAG-GGGAAAATTAAGGCGGTCCCAAAAGTCATGCAG-CGGGGGAAAATTTTCAGCGGGGGCCCCTGGTG-

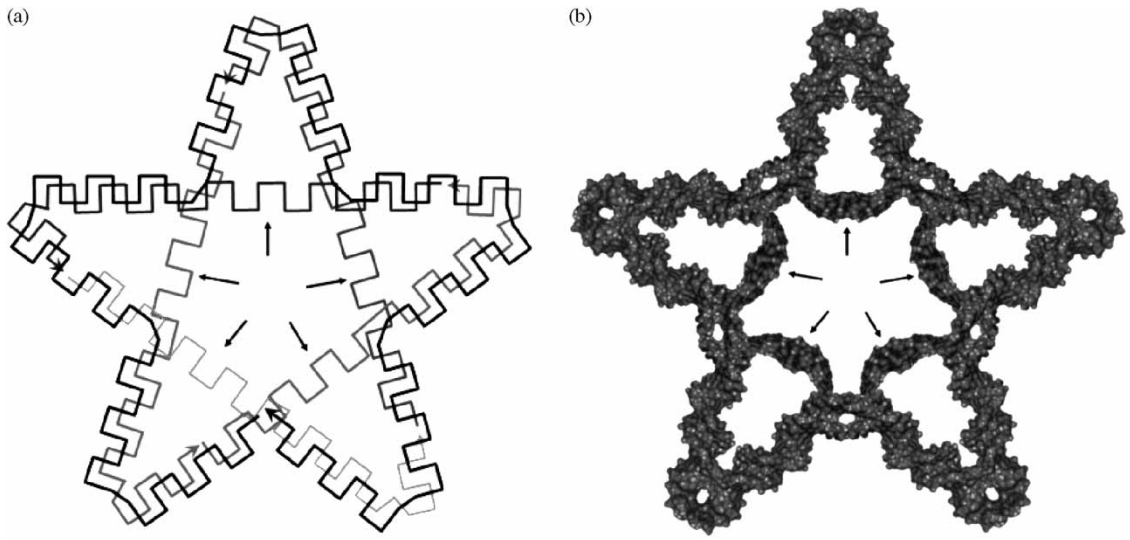

Figure 2. 5-Point star shape DNA nano gear. (a) The schematic view of six ssDNAs which bind with good fidelity and form a 5-point star shape structure. (b) The modeled structure which is consisted of those six ssDNAs. The 5-point star shape structure includes five arms and five linker domains (pointed with the arrows) at the center of the structure.

CACCGGAAATTTCCCCCATATGGGTCGGTTCCTG-GATTTGTGTTAG-3′

D; 5′-GCACTGGCATCCTACTGAAAATTTTCCCC-CTTCGCAACAACACACGCCTTAATTTTCCCCAAA-AAAAAAAAAAAAATTCCCAAACTAACACCCCCCC-CCCCCCCCCCATGGGGGAAATTTCC-3′

Again, the first sequence (A) was main sequences and it was longer than the others, while the last sequence (D) was the shortest sequence and it was the supporter sequence. There was no internal complementarity in each sequence, but special domain of each sequence was complementary with another domain of one of the other sequences. The result was formation of an 8-point star shape structure with eight arms. However, in this case there was no linker domain in the final structure. The resulted structure is illustrated in figure 3.

3.1.2 The second method. *General*. In all cases the sequences were consisted of poly-purine domain followed by five A, T, G or C followed by poly-pyrimidine domain and vise versa. The numbers of purine bases in poly-purine were equal to the numbers of pyrimidine bases in the poly-pyrimidine domain. The poly-purine and poly-pyrimidine domains were complementary and would cohere with good fidelity, thus formation of hairpin was common. In the following sessions the formation of the appropriate structures were based on this method. This method was based on formation of the hairpins, thus we named it HP method.

First structure. In the first structure, the sequence was consisted of mixed combinations of poly-purine, poly-pyrimidine domains. The designed sequence was;

5′-AAAAAAAAAAAAAAAAAAAATTTTTCCCCC-CCCCCCCCCCCCCCCTTTTTGGGGGGGGGGGGG-GGGGGGGTCCTTAAAAAAAAAAAAAAAAAAAA TGGGGTTTTTTTTTTTTTTTTTTTTCCCCTGGGGG-GGGGGGGGGGGGGGGGATTTACCCCCCCCCCCCC-CCCCCCCTTTCCTTTTTTTTTTTTTTTTTTT-3′

The order of domains was as; poly-A, five T, poly-C, five T, poly-G, TCCTT, poly-A, five G, poly-T, CCCCT, poly-G, ATTTA, poly-C, TTTCC and poly-T, respectively. The result was formation of a cross shape structure, which contained two A−T arms and two G−C arms. As it is shown in figure 4, there were four linker domains at the center of the structure. Those domains were designed to be used as linkers to join other structures; it would occur using their complementary sequences. Thus the whole structure would join other structures in nanoscale devices and machines. Additionally there were three loops in the structure which would bind other structures using complementarity features. Those loops would be also useful in nano-devices, as sticky arms.

Second structure. In the second structure, the sequences were consisted of two poly-guanine, poly-cytosine domains, plus linker and tail sequences. The designed sequences were;

A; 5′-GGAGTAAAAAGGGGGGGGGTTTTTCCC-CCCCCCCAAAAAGTACG-3′

B; 5′-CGTACAAAAAGGGGGGGGGAACAACCC-CCCCCCCAAAAACTGAC-3′

C; 5′-GTCAGAAAAAGGGGGGGGGTTGTTCCC-CCCCCCCAAAAAGTAGG-3′

D; 5′-CCTACAAAAAGGGGGGGGGAAAAACCC-CCCCCCCAAAAACACTG-3′

E; 5′-CAGTGAAAAAGGGGGGGGGTTCTTCCC-CCCCCCCAAAAAACGTG-3′

The order of domains was as; 5′ tail (five bases), linker (AAAAA), poly-G, loop bases (poly A/T), poly-C, linker and 3′ tail (five bases), respectively. Each of those ssDNAs would form a double stranded arm with a loop and two single stranded tails which contained linkers. Again, here the bases of the loops would be useful in nano-devices, as

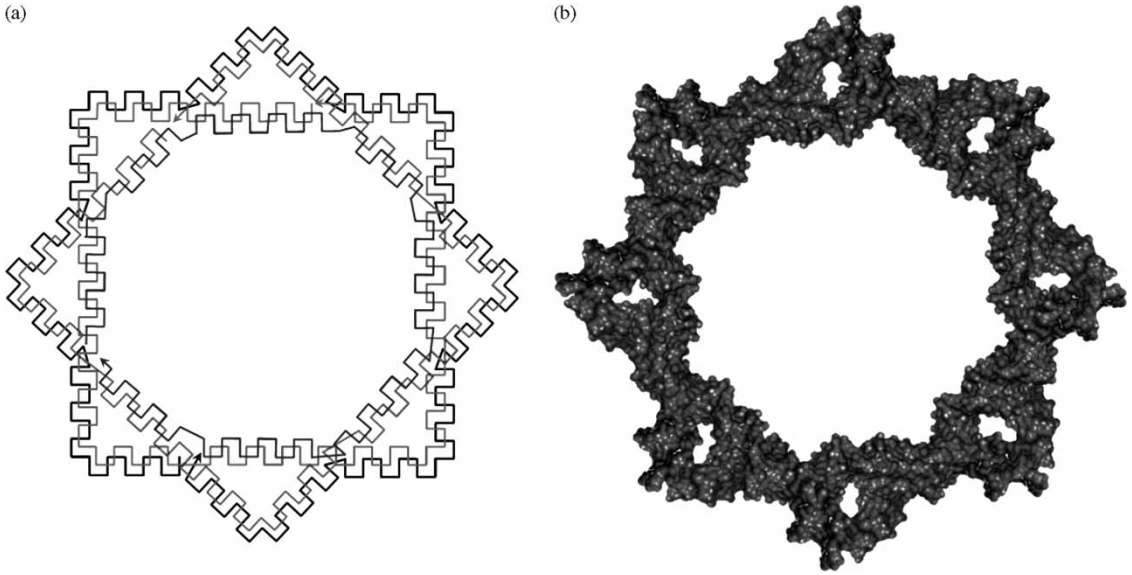

Figure 3. 8-Point star shape DNA nano gear. (a) The schematic view of four ssDNAs which bind with good fidelity and form a 8-point star shape structure. (b) The modeled structure which is consisted of those four ssDNAs. The 8-point star shape structure includes eight arms.

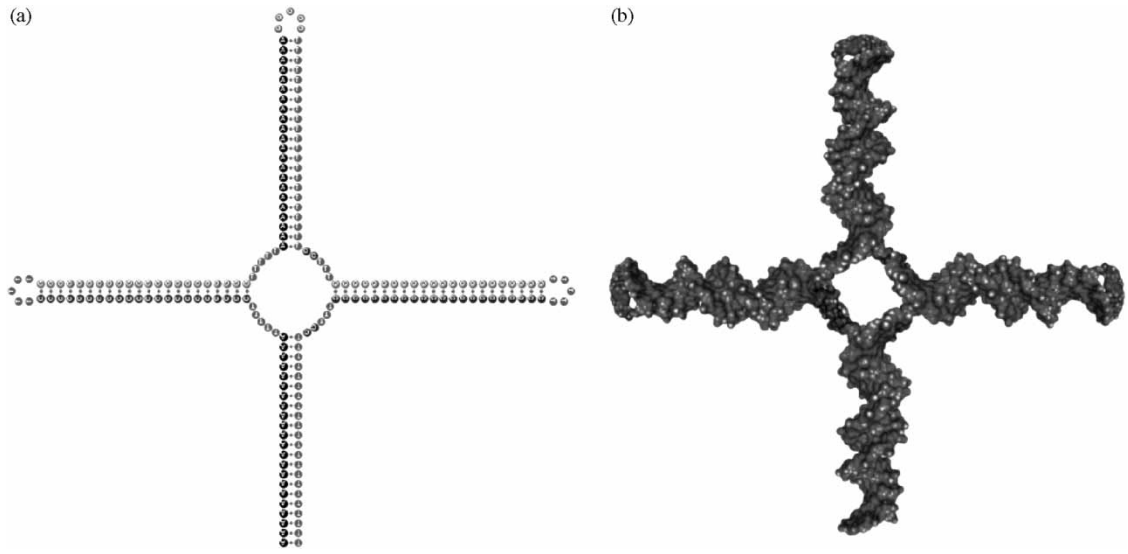

Figure 4. 4-Point cross-shape DNA nano gear. (a) The schematic view of one ssDNA which each domain of it binds to the complementary one. Red, black, blue and brown bales are Thymine (T), Adenine (A), Guanine (G) and Cytosine (C) bases, respectively. (b) The modeled structure which is consisted of the ssDNA. The 4-point cross shape structure includes four arms and four linker domains at the center of the structure. The linker domains were designed to be used as linkers to join other structures; it would occur using their complementary sequences.

sticky arms, and the linker domains would be joining point of the final structure. Against the previous structure, in this case, each of those mentioned sequences has formed a single arm. The final structure was resulted by joining of all single arms together via complementary tails. The final structure was a five arms union, as it is shown in figure 5.

Third structure. In the third structure, the sequences were consisted of two poly-guanine, poly-cytosine domains, plus linker and tail sequences. The designed sequences were;

A; 5′-GGAGTAAAAAGGGGGGGGGGTTTTTCCC-CCCCCCCAAAAAGTACG-3′

B; 5′-CGTACAAAAAGGGGGGGGGGAAAAACCC-CCCCCCCAAAAACTGAC-3′

C; 5′-GTCAGAAAAAGGGGGGGGGGTTTTTCCC-CCCCCCCAAAAAGTAGG-3′

D; 5′-CCTACAAAAAGGGGGGGGGGAAAAACCC-CCCCCCCAAAAACACTG-3′

E; 5′-CAGTGAAAAAGGGGGGGGGGTTTTTCCC-CCCCCCCAAAAAACGTG-3′

F; 5′-CACGTAAAAAGGGGGGGGGGAAAAACCC-CCCCCCCAAAAACTCGT-3′

G; 5′-ACGAGAAAAAGGGGGGGGGGTTTTTCCC-CCCCCCCAAAAAGCAGT-3′

H; 5′-ACTGCAAAAAGGGGGGGGGGAAAAACC-CCCCCCCCAAAAACCTCA-3′

The method which has used for this structure was alike the previous session (second structure), unless the number

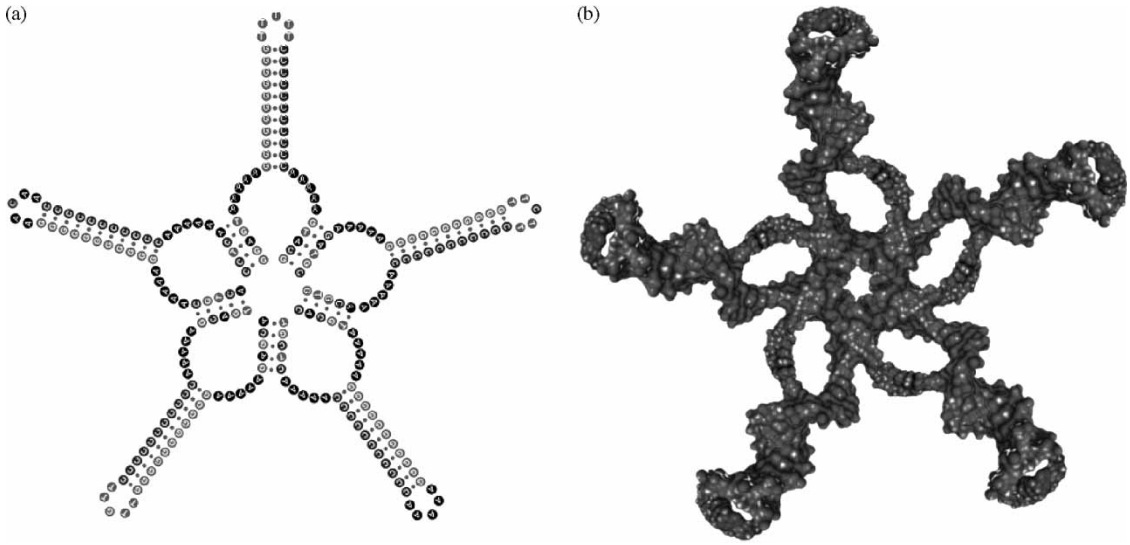

Figure 5. 5-Point cross shape DNA nano gear. (a) The schematic view of five ssDNAs. Red, black, blue and brown bales are Thymine (T), Adenine (A), Guanine (G) and Cytosine (C) bases, respectively. (b) The modeled structure which is consisted of the ssDNA. The 5-point cross shape structure includes five arms and five linker domains at the center of the structure.

of arms were eight. The final structure was resulted by joining of all single arms together via complementary tails. The final structure was an eight arms union, as it is shown in figure 6.

Forth structure. In the forth structure the sequences were consisted of two poly-guanine, poly-cytosine domains, plus tail sequences. The designed sequences were;

A; 5′-GGAGTGGGGGGGGGGTTTTTCCCCCCCCC-CCGTACG-3′

B; 5′-CGTACGGGGGGGGGGAAAAACCCCCCCCC-CCCTGAC-3′

C; 5′-GTCAGGGGGGGGGGGTTTTTCCCCCCCCC-CGTAGG-3′

D; 5′-CCTACGGGGGGGGGGAAAAACCCCCCCCC-CCCACTG-3′

E; 5′-CAGTGGGGGGGGGGGTTTTTCCCCCCCCC-CCGTG-3′

F; 5′-CACGTGGGGGGGGGGAAAAACCCCCCCCC-CCCTCGT-3′

G; 5′-ACGAGGGGGGGGGGGTTTTTCCCCCCCCC-CCGCAGT-3′

H; 5′-ACTGCGGGGGGGGGGAAAAACCCCCCCC-CCCCTCA-3′

Again the method was alike the previous session (third structure), except there were no linker domains in the sequences. The final structure was resulted by joining of all single arms together via complementary tails. The final structure was an eight arms union, as it is shown in figure 7.

3.2 Thermodynamics of the sequences

The thermodynamics of each junction in the structures were calculated and the results are inputted in the table 2. Table 2 includes the calculated thermodynamics both in single junction formation and also the energy changes of binding the junctions together. The T_m of each structure was also calculated (table 2). The results indicated that formation of each structure is spontaneous. Additionally, the predicted structures had contained the least free energy among all possible conformations and thus were the most stable conformations; the less free energy, the more stability of the structure.

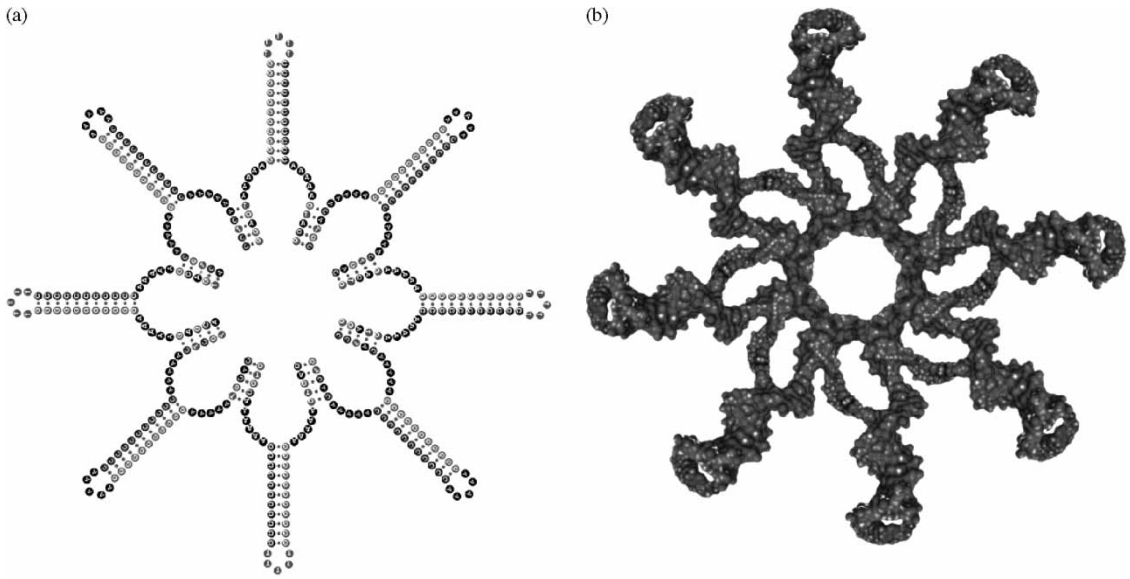

Figure 6. 8-Point cross shape DNA nano gear with linker domains. (a) The schematic view of eight ssDNAs. Red, black, blue and brown bales are Thymine (T), Adenine (A), Guanine (G) and Cytosine (C) bases, respectively. (b) The modeled structure which is consisted of the ssDNA. The 8-point cross shape structure includes eight arms and eight linker domains at the center of the structure.

Table 2. ΔH°, ΔS°, ΔG° and T_m for formation each structure. All values refer to forming duplex at 1M NaCl, 25°C, and pH = 7.0. The 8-Point Cross 1 refers to the 8-Point Cross shape gear which included the linker domains and the 8-Point Cross 2 is 8-Point Cross shape gear which didn't include the linker domains.

Structure	*ΔH° kcal/mol*	*ΔS° Kcal/K·mol*	*ΔG° kcal/mol*	T_m °C
4-Point Star	− 1477.3	− 3.95418	− 250.91	98.7
5-Point Star	− 2089.4	− 5.55918	− 365.22	101.5
8-Point Star	− 2304.2	− 6.12955	− 403.12	100.55
4-Point Cross	− 643.6	− 1.7728	− 93.75	89.8
5-Point Cross	− 639.2	− 1.70165	− 111.31	101.15
8-Point Cross 1	− 998.6	− 2.6704	− 170.19	104.15
8-Point Cross 2	− 957	− 2.5548	− 164.47	105.4

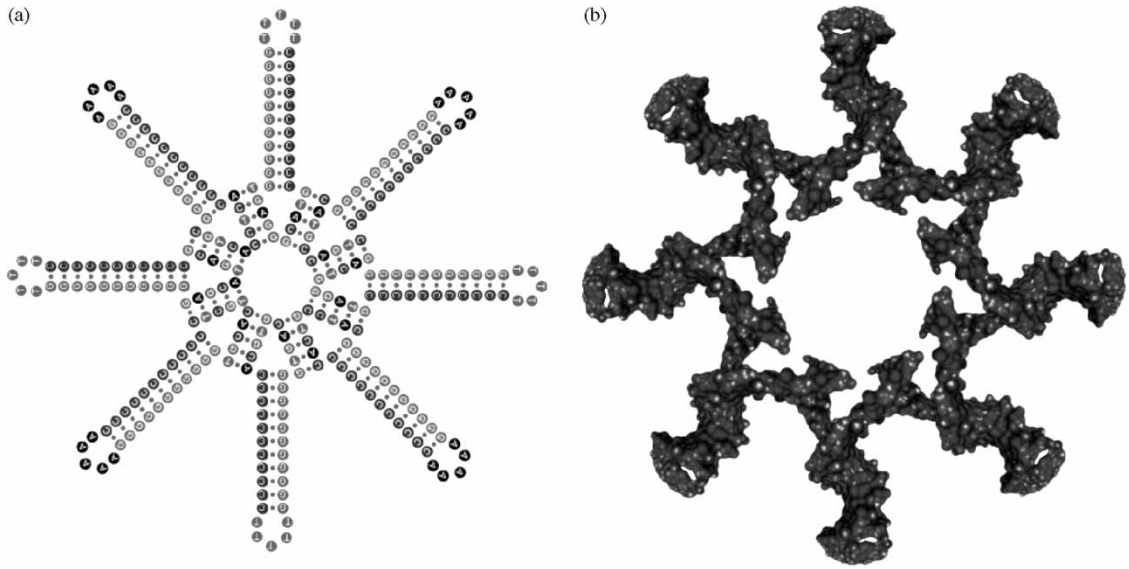

Figure 7. 8-Point cross shape DNA nano gear without linker domains. (a) The schematic view of eight ssDNAs. Red, black, blue and brown bales are Thymine (T), Adenine (A), Guanine (G) and Cytosine (C) bases, respectively. (b) The modeled structure which is consisted of the ssDNA. The 8-point cross shape structure includes eight arms.

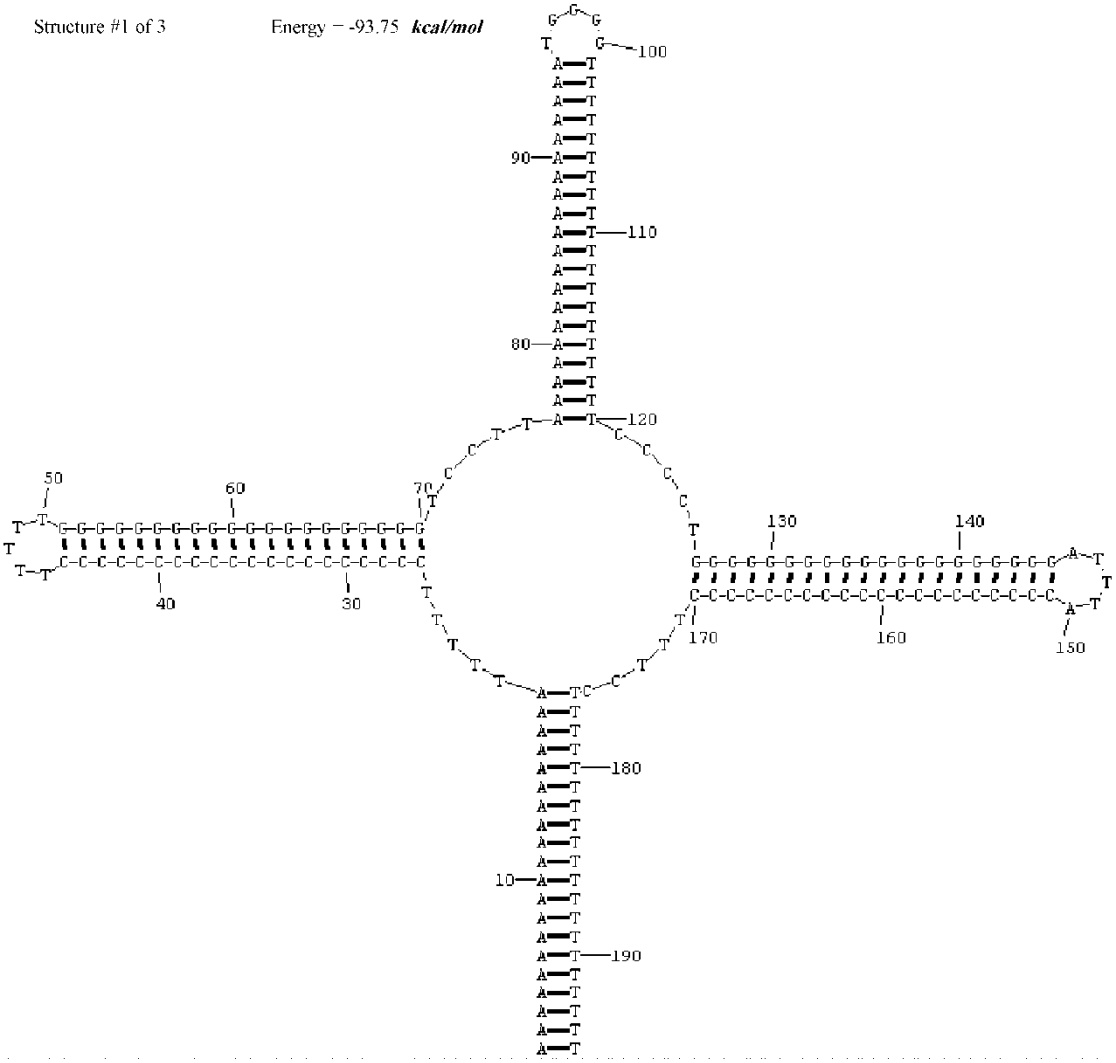

Figure 8. The first predicted 4-Point Cross- shape structure. This structure possesses the least ΔG (−93.75 kcal/mol) among all three possible structures, therefore it is the most probable and the most stable structure. Other possible structures are shown in the figures 9 and 10.

To test the results accuracy, we have used some previously published programs [33–35]. The results, including the T_m and thermodynamics, were confirmed by those programs. It should be noted that the mentioned structures form with the lowest free energy. Even the final structures are desired and posses the lowest free energy, there are other possible structures too. But their possibilities to form are less than of final desired structures. Each possible conformation for the final structures was studied, and the structures with the lowest free energy were assumed as the final structure. For example, in the second method for the first structure, three parallel structures would form, as the whole ssDNA would fold in various patterns. But the desired structure posses the lowest free energy (see figures 8–10 for more information).

3.3 Dimensions of the structures

The dimensions of each structure were calculated. For the 4-point star the distance between two adjacent arm tips was as $\chi_1 = 0.085n(\cos_{33.75^\circ})$nm, and the diameter of whole structure (end to end) was as $\chi_2 = 0.085n(\cos_{22.5^\circ} \times \sqrt{2})$nm, where as n is the number of bases of the strand A (the longest strand). As the longest strand was consisted of 180 bases, therefore, $\chi_1 = 12.72$ nm and $\chi_2 = 19.99$ nm, respectively. For the 5-point star the distance between two adjacent arm tips was as$\chi_1 = 0.034n\sqrt{2 + \sin_{18^\circ}}$ nm, and the diameter of whole structure (end to end) was as$\chi_2 = 0.068n(1 + \sin_{18^\circ})$ nm, where as n is the number of bases of the strand A (the longest strand). As the longest strand was consisted of 250 bases therefore $\chi_1 = 12.92$ nm and $\chi_2 = 22.25$ nm, respectively. For the 8-point star the distance between two adjacent arm tips was as$\chi_1 = 0.02125n \times \sqrt{3/2}$ nm, and the diameter of whole structure (end to end) was as$\chi_2 = 0.0425n \times (1 + 2/\sqrt{2})$ nm, where as n is the number of bases of the strand A (the longest strand). As the longest strand was consisted of 160 bases therefore $\chi_1 = 4.16$ nm and $\chi_2 = 16.42$ nm, respectively.

For the 4-point cross the distance between two adjacent loops was as$\chi_1 = 0.34n \times \sqrt{2}$ nm, and the diameter of whole structure (end to end) was as$\chi_2 = 0.085m$ nm, where as n and m are the number of first poly-A bases and the number of total bases of the strand, respectively. As n was 20, therefore, $\chi_1 = 9.62$ nm and as m was 195 therefore $\chi_2 = 16.58$ nm. For the 5-point cross the distance between two adjacent loops was as $\chi_1 = 0.34n \times \sin_{36^\circ}$ nm, and the diameter of whole structure (end to end) was as $\chi_2 = 0.17n(1 + 2\sin_{36^\circ})$nm, where as n is the number of bases of each strand. As each strand was consisted of 45 bases therefore $\chi_1 = 8.99$ nm and $\chi_2 = 16.64$ nm, respectively. For both 8-point crosses the distance between two adjacent loops was as$\chi_1 = (0.17n \times \sqrt{1 + \sin_{45^\circ}}) - 1.7$ nm, and the diameter of whole structure (end to end) was as $\chi_2 = [0.34n \times (1 + \sin_{45^\circ})] - 3.4$ nm, where as n is the number of each ssDNA bases. For the first 8-point Cross

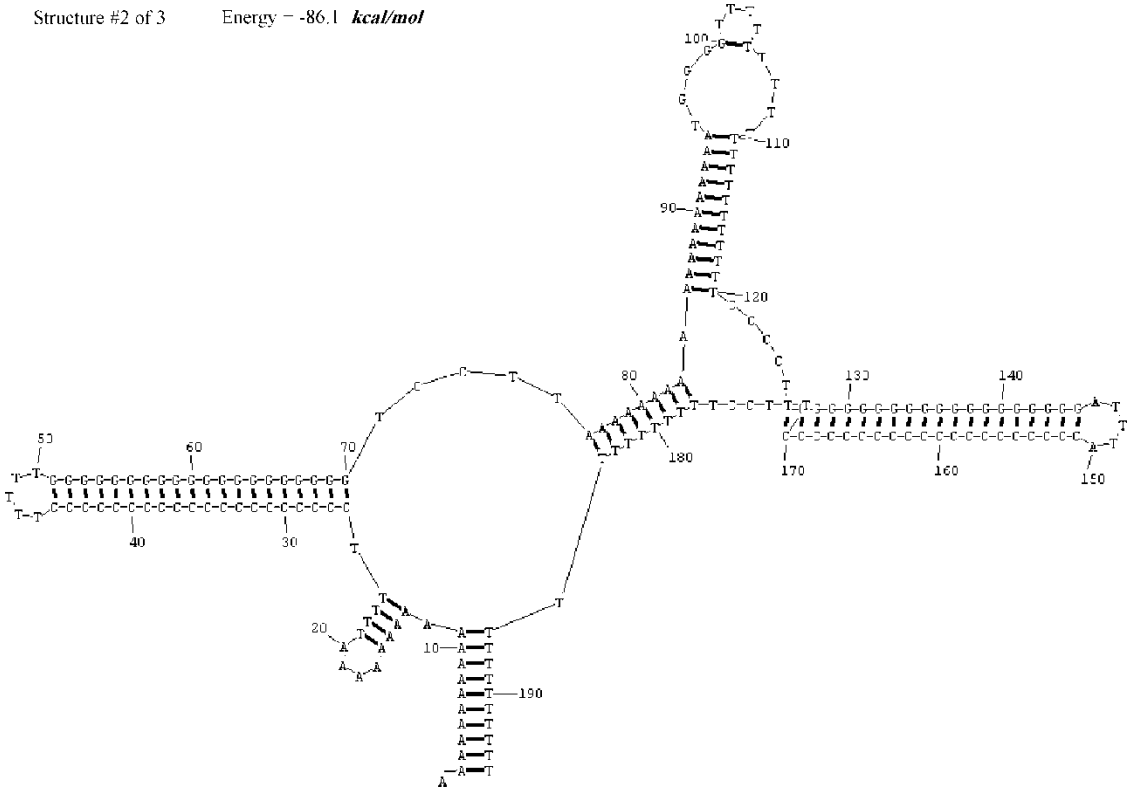

Figure 9. The second predicted 4-Point Cross- shape structure. This structure possesses ΔG of − 86.1 kcal/mol.

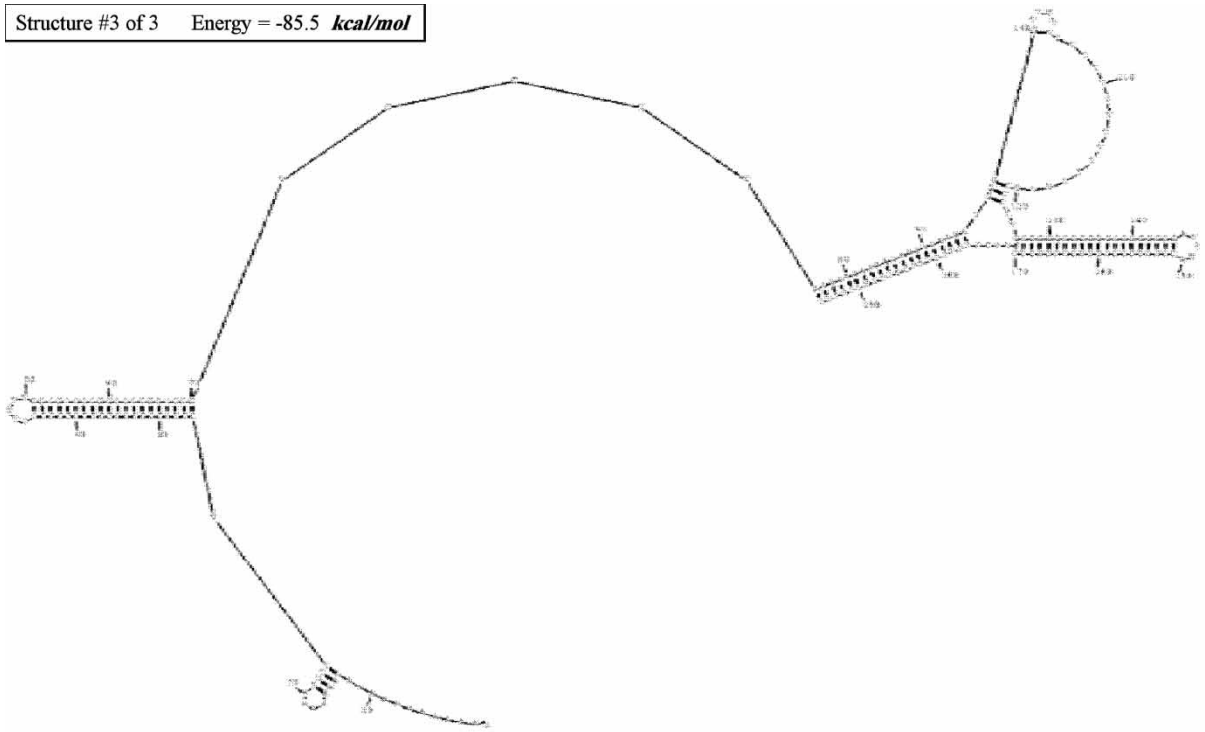

Figure 10. The third predicted 4-Point Cross- shape structure. This structure possesses ΔG of −85.5 kcal/mol.

structure as n was 45, therefore, $\chi_1 = 11.36$ nm and $\chi_2 = 22.72$ nm. For the second 8-point cross structure as n was 35, therefore, $\chi_1 = 6.07$ nm and $\chi_2 = 16.91$ nm.

4. Discussion

DNA self-assembly is the most advanced and versatile system that has been experimentally demonstrated for programmable construction of patterned systems on the nano-scale. In this study we designed a new method to construct fully designed nano-gears using DNA nano-technology. Many nanoscale structures can be made using such special gears. The most important impact of these kinds of structure is that they are self assembler.

Two different approaches to DNA based nano structure construction, DNA templates and DNA hairpins, were studied in the present work. The results indicated that both two methods were successful and useful, even the structures which were resulted of the first method were more stable as their free energy were less. However, it is easier to design sequences for the second method. The most important key point here is to design accurate sequences, as the folding process is very sensitive to the free energy and the accuracy of the base pairing with the least mismatches.

One of the most valuable benefits of construction such gears is their use in nano-machines and nano-motors. Additionally, as those structures are intelligent, they would find their proper position simply. We designed the system to grant this criterion; there were some linker domains which would bind other structures. These kinds of nanostructures, nano-gears, are fundamental for the development of future useful molecular-level devices, as traditional top-down fabrication methods for manufacturing such devices will reach their resolution limits at close future.

Acknowledgements

We thank Professor Afsaneh Safavi, Professor Mahmud Barati Khajoee, Dr Hassan Mohabatkar and Dr Hossein Sabzyan for their comments on the subject, Dr Ali Asgar Amiri, Dr. Elahe Farjami and Mrs Lalaeh Rafiee for their helpful discussions on the manuscript. Dedicated to Professor Nadrian C. Seeman.

References

[1] A. Turberfield. DNA as an engineering material. *Phys. World*, **16**, 43 (2003).
[2] N.C. Seeman. DNA in a material world. *Nature*, **421**, 427 (2003).
[3] R. Mohammadzadegan, H. Mohabatkar. Computer-aided design of nano-filter construction using DNA self-assembly. *Nanoscale Res. Lett.*, **2**, 24 (2007).
[4] R. Mohammadzadegan, M.H. Sheikhi. Applicable DNA nanonetworks. *J. Comput. Theor. Nanosci.*, (2007) Article in press.
[5] R. Mohammadzadegan, M.H. Sheikhi. An ultra-sensitive nanosensor to detect HIV-1. *J. Comput. Theor. Nanosci.*, (2007) Article in press.
[6] C.M. Niemeyer, B. Ceyhan. DNA-directed functionalization of colloidal gold with proteins. *Angew. Chem. Int. Ed. Engl.*, **40**, 3685 (2001).
[7] C.M. Niemeyer, C.A. Mirkin (Eds.). *Nanobiotechnology: Concepts, Applications and Perspectives*, Wiley-VCH, Weinheim (2004).
[8] J.J. Storhoff, C.A. Mirkin. Programmed materials synthesis with DNA. *Chem. Rev.*, **99**, 1849 (1999).
[9] J. Wengel. Nucleic acid nanotechnology-towards Angstrom-scale engineering. *Org. Biomol. Chem.*, **2**, 227 (2004).

[10] N.C. Seeman. Nucleic acid nanostructures and topology. *Angew. Chem. Int. Ed. Engl.*, **37**, 3220 (1998).
[11] N.C. Seeman. In the nick of space: generalized nucleic acid complementarity and the development of DNA nanotechnology. *Synlett*, **2000**, 1536 (2000).
[12] W.M. Shih, J.D. Quispe, G.F. Joyce. A 1.7-kilobase single-stranded DNA that folds into a nanoscale octahedron. *Nature*, **427**, 618 (2004).
[13] H. Li, S.H. Park, J.H. Reif, T.H. LaBean, H. Yan. DNA-templated self-assembly of protein and nanoparticle linear arrays. *J. Am. Chem. Soc.*, **126**, 418 (2004).
[14] E. Winfree, F. Liu, L.A. Wenzler, N.C. Seeman. Design and self-assembly of two-dimensional DNA crystals. *Nature*, **394**, 539 (1998).
[15] H. Yan, T.H. LaBean, L. Feng, J.H. Reif. Directed nucleation assembly of DNA tile complexes for barcode-patterned lattices. *Proc. Natl. Acad. Sci. USA*, **100**, 8103 (2003).
[16] H. Yan, S.H. Park, G. Finkelstein, J.H. Reif, T.H. LaBean. DNA-templated self-assembly of protein arrays and highly conductive nanowires. *Science*, **301**, 1882 (2003).
[17] J. Shi, D.E. Bergstrom. Assembly of novel DNA cycles with rigid tetrahedral linkers. *Angew. Chem. Int. Ed. Engl.*, **36**, 111 (1997).
[18] S.M. Waybright, C.P. Singleton, K. Wachter, C.J. Murphy, U.H.F. Bunz. Oligonucleotide-directed assembly of materials: defined oligomers. *J. Am. Chem. Soc.*, **123**, 1828 (2001).
[19] J.L. Czlapinski, T.L. Sheppard. Template-directed assembly of metallosalen-DNA hairpin conjugates. *ChemBioChem*, **5**, 127 (2004).
[20] Z.J. Gartner, M.W. Kanan, D.R. Liu. Expanding the reaction scope of DNA-templated synthesis. *Angew. Chem. Int. Ed. Engl.*, **41**, 1796 (2002).
[21] J.J. Li, W. Tan. A single DNA molecule nanomotor. *Nano Lett.*, **2**, 315 (2002).
[22] C. Mao, W. Sun, Z. Shen, N.C. Seeman. A nanomechanical device based on the B–Z transition of DNA. *Nature*, **397**, 144 (1999).
[23] B. Yurke, A.J. Turberfield, A.P. Mills, J.F.C. Simmel, J.L. Neumann. A DNA-fuelled molecular machine made of DNA. *Nature*, **406**, 605 (2000).
[24] H. Yan, X. Zhang, Z. Shen, N.C. Seeman. A robust DNA mechanical device controlled by hybridization topology. *Nature*, **415**, 62 (2002).
[25] J. SantaLucia. A unified view of polymer, dumbbell, and oligonucleotide DNA nearest-neighbor thermodynamics. *Proc. Natl. Acad. Sci. USA*, **95**, 1460 (1998).
[26] I. Tinoco Jr., C. Bustamante. How RNA folds. *J. Mol. Biol.*, **293**, 271 (1999).
[27] N.C. Seeman. *De novo* design of sequences for nucleic acid structural engineering. *J. Biomol. Struct. Dyn.*, **8**, 573 (1990).
[28] J.D. Puglisi, I. Tinoco Jr. (Eds.), methods in Enzymology, Academic Press, San Diego, CA (1989).
[29] C.E. Mortimer. *Chemistry*, Wadsworth Publishing, Belmont, CA (1986).
[30] Y. Li, G. Zon, W.D. Wilson. Thermodynamics of DNA duplexes with adjacent G.A mismatches. *Biochemistry*, **30**, 7566 (1991).
[31] I. Kollosvary, W.C. Guida. Torsional flexing: conformational searching of cyclic molecules in biased internal coordinate space. *J. Comput. Chem.*, **14**, 691 (1993).
[32] W. Humphrey, A. Dalke, K. Schulten. VMD-visual molecular dynamics. *J. Mol. Graphics*, **14**, 33 (1996).
[33] M. Zuker. Mfold web server for nucleic acid folding and hybridization prediction. *Nucleic Acids Res.*, **31**, 3406 (2003).
[34] P. De Rijk, R. De Wachter. RnaViz, a program for the visualisation of RNA secondary structure. *Nucleic Acids Res.*, **25**, 4679 (1997).
[35] D.H. Mathews, M.D. Disney, J.L. Childs, S.J. Schroeder, M. Zuker, D.H. Turner. Incorporating chemical modification constraints into a dynamic programming algorithm for prediction of RNA secondary structure. *Proc. Natl. Acad. Sci. USA*, **101**, 7287 (2004).